Molecular Insights on the Dihydrogen Bond Properties of Metal Borohydride Complexes upon Ammoniation

ECS Journal of Solid State Science and Technology, 2021 **10** 091006
2162-8777/2021/10(9)/091006/9/$40.00 © 2021 The Electrochemical Society ("ECS"). Published on behalf of ECS by IOP Publishing Limited

Molecular Insights on the Dihydrogen Bond Properties of Metal Borohydride Complexes upon Ammoniation

Saravanapriya Arumugam,[1,2] Abiram Angamuthu,[3] and Praveena Gopalan[1,z]

[1]*Department of Physics, PSGR Krishnammal College for Women, Coimbatore 641004, India*
[2]*Department of Physics, Dr. N.G.P Arts and Science College, Coimbatore 641048, India*
[3]*Department of Physics, Karunya Institute of Technology and Sciences, Coimbatore 641114, India*

The dihydrogen bond (DHB) that exists between BH···HN containing systems is known for the improved thermodynamic properties of complex hydrides. This study explores the stability and electronic properties of dihydrogen bonds ($H^{\delta-}\cdots H^{\delta+}$) that exist between the protic hydrogen, $H^{\delta+}$ in NH_3 and hydridic hydrogen, $H^{\delta-}$ of BH_4 in AMgB···MB and AMgB···AMB complexes (where M = Li, Na, K, Mg and Zn; and A = Amino group) using second order Moller-Plesset perturbation theory (MP2). The effect of metals and ammoniation in varying the nature of the DHB was revealed in quantum theory of atoms in molecule (QTAIM) analysis with the identification of non-covalent interactions. The calculated values of interaction energies were correlated well with the topological results. Furthermore, energy decomposition analysis (EDA), interaction energy and Bader charge analysis were calculated in order to interpret the role of non-bonded interaction on decomposition process. The calculated structural, QTAIM and EDA analysis reveal the presence of non bonded interaction in all the complexes. Overall analysis of the study reported that the process of adding amine group in alkali metal borohydrides increases charge distribution around the dispersion interaction which plays a vital role in hydrogen evolution process.
 [DOI: 10.1149/2162-8777/ac232a]

Manuscript submitted May 5, 2021; revised manuscript received August 26, 2021. Published September 14, 2021. *This paper is part of the JSS Focus Issue on Selected Papers from the International Conference on Nanoscience and Nanotechnology 2021 (ICONN-2021).*

Supplementary material for this article is available online

Dihydrogen bond (DHB), an electrostatic interaction that takes place between a protonic hydrogen and a hydridic hydrogen is considered as a new valuable approach for tailoring material properties.[1] DHBs allow a rapid self-organization of molecular building blocks into extended regular structures with well-defined physical and chemical properties.[2–5] In metal hydrides, dihydrogen bonds were found to control the hydride structure and reactivity and also affect the selectivity of reactions such as hydrogen exchange, alcoholysis, aminolysis, hydrogen evolution, double-bond reduction and cleavage reactions.[6] Most importantly, the DHBs were also found to be the plausible intermediates that promote proton/hydride exchange and elimination of molecular hydrogen formation in various metal hydride systems. For instance, Golub et al. established the dimerization process of transition metal tetrahydroborate interaction with wide range of proton donors and they reported the formation of DHB intermediates with the release of hydrogen both the experimentally and theoretically.[7] Subsequent analysis of the aforementioned research group shed light into the influence of DHBs as well as the nature of metal atom on H_2 evolution in monodentate tetrahydroborate complexes.[7–9] DHBs also exist between different metal hydrides that satisfy the criteria of forming stable crystal structures. In this row, the light metal borohydrides $M(BH_4)_n$ (M = alkaline or alkaline earth metals) are a class of compounds that have gained significant position in solid state hydrogen storage owing to their high gravimetric and volumetric hydrogen densities.[10]

Though research in metal borohydrides for hydrogen storage shows a promising progress, shortcomings such as higher dehydrogenation temperatures, sluggish dehydrogenation kinetics, poor cyclic reversibility and the presence of impurities in the released hydrogen still exist.[10] Furthermore, most of the studies on $M(BH_4)_n$ (e.g., M = Zn, Al, Ti, Mn and Zr) were found to be irreversible due to their low melting temperatures and also demonstrated the release of diborane with hydrogen.[11–15] Consequently, there are studies that have focused on the importance of DHB in enhancing the hydrogen storage properties of MBHs. Quite a number of efforts[16–18] have also been devoted on $M(BH_4)_n$ systems to reduce their thermodynamic stability and to overcome the kinetic barriers. The research of AMBs as potential hydrogen storage materials was initiated by Soloveichik et al. wherein they demonstrated the importance of DHB in decreasing the decomposition temperature of AMB systems.[19] Further, a pioneering work on the interaction of B-H···H-N in Amine Metal Borohydrides (AMB) by Jensen et al. has shown improved thermodynamics in which dehydrogenation was resulted from the $N–H^{\delta+}\cdots^{\delta-}H–B$ type of interactions.[20] Aforementioned research group of Torben R Jensen were well explored the importance of DHB interaction through both the experimental as well as theoretical observations in various AMB systems like $LiBH_4.\frac{1}{2}NH_3$ and $Mg(BH_4)_2.NH_3$ in which the existence of DHB play an important role in its structural stability in the solid state and also for the cation conductivity.[21,22] Subsequently, when compared to alkali and alkali-earth metal borohydride systems, several experimental studies[23–26] have shown the presence of $N–H^{\delta+}\cdots^{\delta-}H–B$ dihydrogen bonds in AMB compounds facilitating hydrogen splitting and considerably decreasing the dehydrogenation temperatures by about 60°C–250°C. So far, various ammoniated metal borohydrides such as $LiBH_4.NH_3$,[27] $Al(BH_4)_3.nNH_3$,[28] $LiMg(BH_4)_3.2NH_3$[29] and $M(BH_4)_2.2NH_3$[30–32] (M = Mg, Ca, Zn) were reported to be the potential candidates for hydrogen storage with reduced decomposition temperature.

Though quite a number of experimental and theoretical studies have been made on analyzing the role of DHB in various metal borohydride systems,[33–36] molecular level insights on the tuning of $N–H^{\delta+}\cdots^{\delta-}H–B$ dihydrogen bonds in metal borohydrides upon ammoniation and their role in hydrogen decomposition properties are almost absent in the literature.[37] Hence, this work aims to provide the quantum mechanical aspects of $N–H^{\delta+}\cdots^{\delta-}H–B$ dihydrogen bonds in various metal borohydrides (MB) systems on the basis of ammoniation. The main drawback of AMB system in general is that they also give undesirable release of ammonia during dehydrogenation.[19] Hence recently, experimental studies are being focused on various AMB···MB mixtures that are shown to tune the H_2 release temperature and purity considerably.[20] Thus, in this context of research, the dependence of dihydrogen bond properties upon ammoniation in AMB···MB and AMB···AMB mixtures will be also analyzed. Further, among the AMBs studied, $Mg(BH_4)_2.2NH_3$ system is found to release H_2 effectively with the hydrogen mass percentage of 13.1. Hence, this study explores mainly the interaction

[z]E-mail: gopalpraveena@gmail.com

of $Mg(BH_4)_2.2NH_3$(AMgB) system with different metal borohydrides $M(BH_4)$ and also with its amine metal borohydride systems $M(BH)_4.NH_3$(where M = Li, Na, K, Mg and Zn). The structure and electronic properties of the dihydrogen bonded $Mg(BH_4)_2.2NH_3$···MB and $Mg(BH_4)_2.2NH_3$···AMB complexes will be explored employing second order Moller-Plesset perturbation theory (MP2). In order to understand the charge transfer of $N–H^{\delta+}···^{\delta-}H–B$ interactions, Bader charge analysis will be performed using QTAIM theory.[38] Interaction energy and EDA analysis of the considered complexes will be evaluated.

System Set-Up and Computational Methodology

Various experimental studies[28,32] have pointed out that circumventing the release of ammonia upon dehydrogenation in AMB systems could be made possible if the ratio between BH_4 and NH_3 is equal to or less than the unity.[20] Thus, in order to maintain the equal composition ratio of BH_4 and NH_3 groups in AMBs, 5 different compounds namely $Li(BH_4).NH_3$, $Na(BH_4).NH_3$, $K(BH_4).NH_3$, $Mg(BH_4)_2.2NH_3$ and $Zn(BH_4)_2.2NH_3$ are considered along with the MB compounds such as $Li(BH_4)$, $Na(BH_4)$, $K(BH_4)$, $Mg(BH_4)_2$ and $Zn(BH_4)_2$, respectively. Further, it is also demonstrated experimentally that ammoniating a metal borohydride would lower the decomposition temperature when metal borohydrides that contain metals of electronegativity $\chi \leqslant 1.6$.[37,39] Thus, the choice of metals in the considered systems is purely based on the dependence of the electronegativity χ of metals. Hence, in the present study the metals such as Li, Na, K, Mg, and Zn with χ values of 0.98, 0.9, 0.82, 1.31 and 1.65 are chosen.[39]

As mentioned earlier, in order to understand the tuning properties of $N–H^{\delta+}···^{\delta-}H–B$ dihydrogen bonds, the aforementioned MB and AMB structures are thus made to interact with $Mg(BH_4)_2.2NH_3$ system. Hence in total, 10 complexes such as AMgB···$Li(BH_4)$, AMgB···$Na(BH_4)$, AMgB···$K(BH_4)$, AMgB···$Mg(BH_4)_2$, AMgB···$Zn(BH_4)_2$, AMgB···$Li(BH_4).NH_3$, AMgB···$Na(BH_4).NH_3$, AMgB···$K(BH_4).NH_3$, AMgB···AMgB and AMgB···$Zn(BH_4)_2.2NH_3$ are considered and analyzed. The construction of the considered molecular isolates and their complexes were made using Chemcraft program package.[40]

Thus, all the structures were optimized at MP2/6–311++G** level of theory with LANL2DZ basis set, solitarily used for metals (M = Li, Na, K, Mg, and Zn).[41] The topological aspects of DHBs in the optimized complexes were made through the analyses of ellipticity, electron density, and Laplacian of electron density using Multiwfn software.[42] The obtained positive vibrational frequencies of all the optimized systems confirm their minima in the potential energy surface. Further, the strength of DHB interactions between the complexes is analyzed with the help of BSSE corrected interaction energies,[43] Energy decomposition analysis[44] and MESP. All the calculations were performed using Gaussian09 program package.[45]

Theoretical Background

Topological analysis.—Electron density ρ(r) at bond critical point and its Laplacians ($\nabla^2\rho$) are important parameters to characterize the nature of bonding.[38] The topological analysis of the complexes was analyzed with the help of QTAIM analysis. Diagonalization of the Hessian of the electron density yields three eigenvalues, $\lambda_1 < \lambda_2 < \lambda_3$ from which one can calculate the ellipticity value. The ellipticity (ε) value measures an extent to which charge is preferentially accumulated. Usually, ε is calculated through Eq. 1 as follows,

$$\varepsilon = \frac{\lambda_1}{\lambda_2} - 1 \qquad [1]$$

Interaction energy.—The interaction energy of two interacting molecules can be defined as,

$$\Delta E = E(\mathrm{AB}) - (E(\mathrm{A}) + E(\mathrm{B})) + BSSE \qquad [2]$$

Where, E(AB) is the energy of the dihydrogen bonded complexes, E(A) and E(B) are the energy of the monomers A and B respectively. Here the interaction energy of the dihydrogen bonded complexes was calculated as the difference between the total energy of the optimized complex and sum of the monomer energies. As ΔE must be corrected to account for basis set super-position errors (BSSE), the BSSE corrections were done by using counterpoise (CP) method.[43]

Energy decomposition analysis.—Electrostatic, Exchange and dispersion term contribute to the total interaction energy, that can be defined as

$$\Delta \mathrm{E_{totint}} = \Delta \mathrm{E_{elstat}} + \Delta \mathrm{E_{ex}} + \Delta \mathrm{E_{orb}} \qquad [3]$$

Where, E_{elstat} is electrostatic interaction term, normally negative if the two fragments are neutral, E_{exch} is exchange repulsion term, which comes from the Pauli repulsion effect and is invariably positive. In Multiwfn these two terms combined together and named as steric term (E_{steric}). E_{orb} in above formula is orbital interaction term, and it can be calculated as follows,

$$\Delta \mathrm{E_{orb}} = \mathrm{E_{SCF,Last}} - \mathrm{E_{SCF,First}} \qquad [4]$$

Therefore, steric term can be evaluated from

$$\Delta \mathrm{E_{steric}} = \Delta \mathrm{E_{totint}} - \Delta \mathrm{E_{orb}} \qquad [5]$$

The dispersion term of the interacting complexes can be obtained using HF method in which the dispersion term is completely missing.

$$\Delta E_{\mathrm{disp}} = \Delta E^{MP2}_{\mathrm{tot\ int}} - \Delta \mathrm{E^{HE}_{totint}} \qquad [6]$$

Where, $\Delta E^{MP2}_{\mathrm{tot\ int}}$ and $\Delta E^{HF}_{\mathrm{tot\ int}}$ are total interaction energies calculated at HF and MP2 levels respectively.[46]

MESP

The electrostatic potential V(r) around a molecule by its nuclei and electrons is an important tool for the analysis understanding the interactive behavior of molecules. Topological parameters of MESP are very useful to identify the region of the electron donating group of an atom as well as the electron accepting group. The electrostatic potential of a molecule, which has an electronic density function ρ(r), is given by

$$V(\boldsymbol{r}) = \sum_{N}^{A} \frac{Z_A}{|\boldsymbol{r} - \boldsymbol{R_A}|} - \int \frac{\rho(\boldsymbol{r}')d^3\boldsymbol{r}'}{|\boldsymbol{r} - \boldsymbol{r}'|} \qquad [7]$$

Where $\rho(\mathbf{r}')$ is a continuous electron density and Z_A is the charge on nucleus of atom A located at a distance $\mathbf{R}_A$.[47] All these calculations are performed with the help of Gaussian 09 program package.

Results and Discussion

Geometrical parameters.—The structural analysis of the considered AMgB···B and AMgB···AMB complexes (M = Li, Na, K, Mg and Zn) optimized at the MP2/6–311++G** level of theory is made through the examination of M–B, B–H and M–H bond lengths as given in Table I and the optimized structures were illustrated in Fig. 1. In the case of AMgB···AMgB upon complexation, the Mg-B (2.229 Å) and Mg-N (2.208 Å) bond lengths were seem to be maintained and the values coincide approximately by the amount of ∼0.19 Å and ∼0.059 Å with the crystallographic data of AMgB as given by Soloveichik et al.[19] In the complex AMgB···AZnB, similar to the experimentally demonstrated structure,[31] the two BH_4

Table I. Geometrical parameters for M-H, B-H, N-H bond distances in Å and B-H···H, N-H···H angles in degrees of the optimized structures at MP2/6–311++G level of theory.**

Metal complexes	Radius	M-B	M-H	B-H	N-H	B-H···H	N-H···H
Mg^{2+}	0.72	2.2–2.4	1.8–2.0	1.2	1.01	109°−114°	158°−170°
Zn^{2+}	0.74	2.3	1.8–2.1	1.2	1.01	99°−131°	153°−172°
Li^{+}	0.76	2.03	1.8–1.9	1.2	1.01	99°−145°	149°−154°
Na^{+}	1.02	2.463	2.2–2.3	1.23	1.02	111°−147°	155°−158°
K^{+}	1.38	2.89	2.6	1.2	1.01	109°−130°	155°−160°

groups of AZnB were found to be bonded to Zn atom via two Zn–H–B bonds (Refer Fig. 1). Furthermore, the observed values of Zn–B and Zn–N bond distances of the order of (2.30 and 2.20 Å) also matches well with the experimental results of AZnB system (Zn–B = 2.28 Å and Zn–N = 2.08 Å). In the case of metal borohydrides (MBs), after complexation with AMgB system, the M–B and M–H bond lengths were found to vary almost linearly with the size of metal as: K < Na < Zn < Mg, which is found to be in good correlation with the previous experimental and theoretical studies wherein they demonstrated the increase of M-B distance with the increase of metal radii.[20,48,49]

It is observed from the optimized structure of AMgB···LiB, Li^{+} ion is coordinated to the $[BH_4]^{-}$ group of MB as well as to AMgB through H^{+} bonding. Further, the Na^{+} ion also forms the bonding with one of the H atom in the $[BH_4]^{-}$ of AMgB. Since the Atomic radii increases on moving from Mg to K, interacting metal to H distance increases which influences in the formation of M-H interaction between the chosen MB and AMgB. Except KBH_4 whose atomic radius is comparatively large, all other interacting MBs forms ionic bonding with the AMgB systems. Whereas in the case of ammoniated alkali metal borohydride systems, ammonia molecule of the alkali metals are not bonded with the interacting AMgB as well as MB systems in all the three metals (Li, Na and K) which shows the possibilities of ammonia emission during the decomposition process in the three systems namely AMgB···ALiB, AMgB···ANaB and AMgB···AKB.

As can be seen from Table I, the bond lengths of B-H and N-H that involve in the dihydrogen bond interactions were found to be increased by the amount of 0.01 Å with respect to those that are not involved in the DHB interaction. Except for B-H and N-H bonds that involve in the dihydrogen interaction, all the other B-H and N-H bond lengths of borohydride and ammonia follow the ideal geometry of NH_3 and BH_4. It follows from Table III that the observed H···H bond distances between B-H and N-H of all the chosen AMgB···MB and AMgB···AMB systems fall in the range of 1.7–2.2 Å which correlate well with the previously reported data of BH···HN DHB system.[31] It is readily seen from the measured bond angles (Table I) that all the dihydrogen bonds exhibit a strong preference for a bent geometry with ∠H···HB typically situated between 95° and 120° and with ∠NH···H lies between 150°–170° respectively.[31] Overall analyses on the structure of obtained AMgB···MB and AMgB···AMB complexes show that the geometries share purely the characteristics of experimentally demonstrated structures with the presence of dihydrogen bonds.

Bifurcated DHBs.—The bifurcated hydrogen bond, that is, the formation of two hydrogen bonds at one center, is a common phenomenon for dihydrogen bonds as well as classical hydrogen bonds. Similar kind of bifurcated DHBs were revealed from the geometry optimization of the AMgB···ALiB and AMgB···ZnB systems. Aforementioned systems shows the presence of bifurcated dihydrogen bonds that formed between one hydride ligand of $[BH_4]^{-}$ in MB (M = Li and Zn) and two proton donating H of NH_3 moieties in AMgB. In both the cases one of the H···H interactions is shorter and linear than the other.

Infrared spectra.—As the formation of dihydrogen bonding results in the modification of N–H and B–H bond lengths, this would also correspond significantly to the changes in the stretching frequencies of such bonds. Hence, the B–H and N–H stretching vibrational frequencies of the optimized complexes were observed and analyzed at MP2/6–31 G* level of theory and the results are tabulated in Table II. It is observed from the results that the B-H stretching vibrations of alkali metal containing AMgB…MB (M = Na, Li and K) systems occur around ∼2300 cm^{-1} and that of transition and alkaline metal AMgB···MB (M = Mg and Zn) complexes occur between ∼2500 and 2600 cm^{-1} respectively. After ammoniation, B-H stretching modes of all the chosen alkali metal complexes shows considerably higher frequencies compared to their metal borohydride complexes. However, the B-H stretching modes of ammoniated AMgB···MgB and AMgB···ZnB complexes are considerably lower when compared to their metal borohydride complexes.

Such a lowering of frequencies indicates that the ammoniated complexes of alkaline and transition metals (Mg and Zn) have weaker B–H bonds, which favor for the effective dehydrogenation process. However, various studies have pointed out that the strength of DHBs will further be reflected in the weakening of both N–H and B–H bonding thorough the lowering of vibrational frequencies.[50] Here, comparing the complexes considered, the ammoniation in metal borohydrides involving Mg and Zn metals weakens the B–H interactions indicating the weakening of B–H bonding and thereby possible dehydrogenation at reduced temperatures for such complexes. The N–H stretching modes of AMBs in the complexes were observed as ∼ 3400 cm^{-1} for symmetric and 3500 $cm^{-1}$for asymmetric modes of vibrations. Furthermore, all the observed B–H and N–H stretching frequencies are comparable with the B-H (ν_s ∼ 2284 cm^{-1}, ν_a ∼ 2376 cm^{-1}) and N–H (ν_s ∼ 3257 cm^{-1}, ν_a ∼ 3317 cm^{-1}) modes of ammonia borane systems demonstrated experimentally.[51,52]

Topological analysis.—In order to understand the nature of DHBs in the complexes, QTAIM parameters such as BCP between two hydrogen atom, electron density (ρ) and its Laplacian ($\nabla^2\rho$) at BCP, total electron energy density H(r), potential electron energy density V(r), kinetic electron energy density G(r) and bond ellipticity (ε) values at the interface between two H atoms that involved in DHBs were calculated at BCP and are tabulated in Table III. The QTAIM molecular graph of selected complexes are shown in Fig. 2 and all the QTAIM maps viewed with VMD[53] software are given in supporting information (Fig. S1 (available online at stacks.iop.org/JSS/10/091006/mmedia)). In topological analysis there are four types of critical points (3.−3), (3,−1), (3,+1) and (3,+3). The first and last types are a maximum or a minimum respectively and the middle ones are saddle points. The (3, −1) critical points are also called bond critical point (BCP). The value of ρ and the sign of $\nabla^2\rho$ at BCP are closely related to bonding strength and bonding type respectively for analogous bonds. Figure 2 clearly demonstrates the existence of a BCP for every dihydrogen bond. The electron density ρ of H···H bonds in DHB systems usually found to fall within the range of 0.002–0.035a.u. The observed electron density ρ of H···H

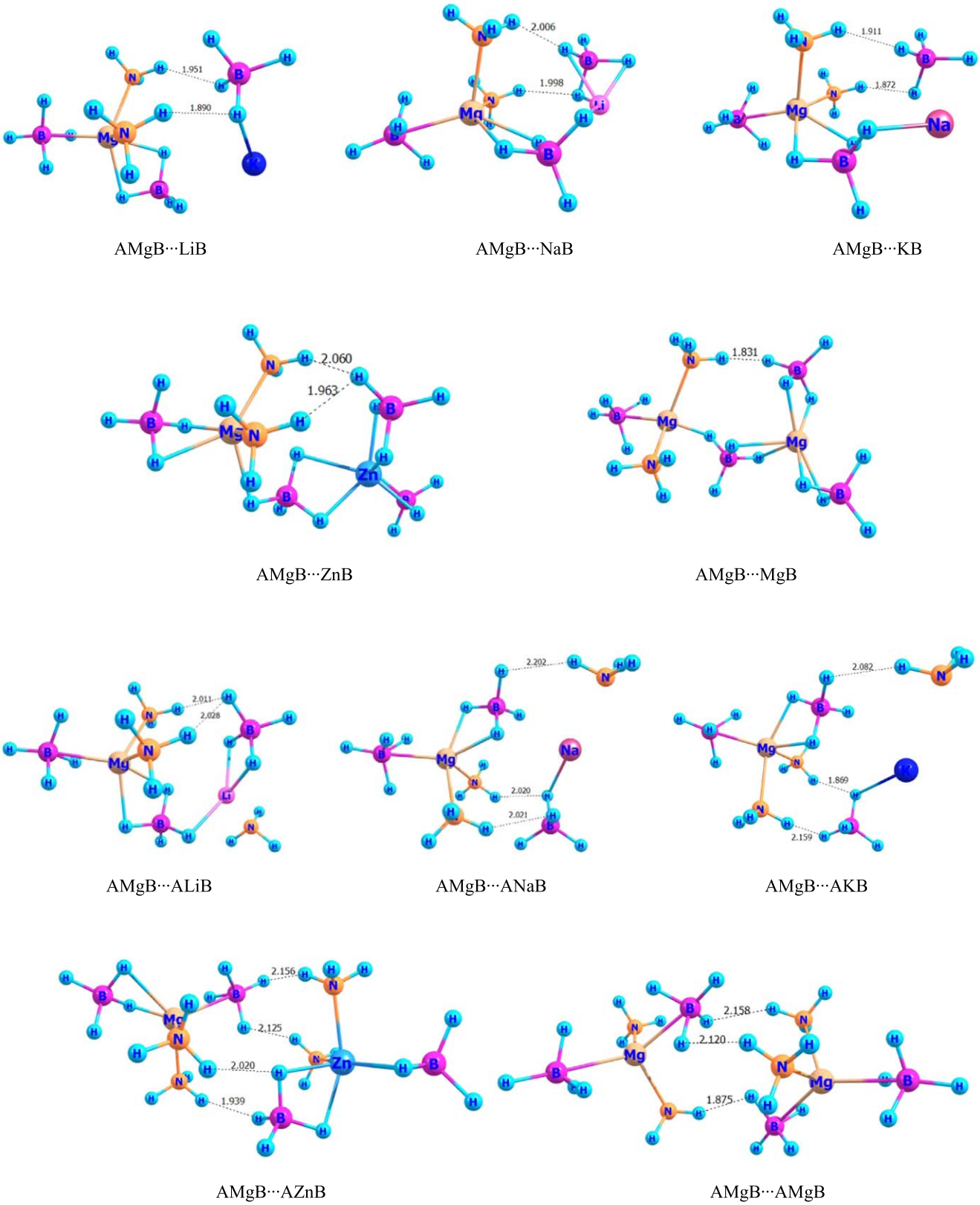

Figure 1. Optimized Structures of AMgB···MB and AMgB···AMB (where M = Li, Na, K, Zn and Mg) complexes at MP2/6–311++G** level of theory.

interactions in the complexes were found to lie between 0.009a.u. and 0.017a.u. respectively. It has been demonstrated theoretically by Popelier[54] that the electron density ρ and bond ellipticity ε at BCP of H···H interactions reveals the strength of DHB interaction. In conjunction with this study, the observed lower value of ρ (0.008a.u.) of H···H in the ANaB containing complex is found to be half by about the observed higher value of ρ (0.017a.u.) in LiB. Such a result reveals further that the DHB of the former to be weaker

Table II. Stretching vibrational frequencies (ν in cm^{-1}) of B-H and N-H bonds involved in DHBs obtained at MP2/6–31 G* level of theory ν^s, ν^a—symmetric and asymmetric modes of vibration.

Amine Metal Borohydride Complexes	B-H Frequency $\nu(cm^{-1})$	N-H Frequency $\nu(cm^{-1})$
AMgB… LiB	2352[a], 2370[a]	3586[a], 3599[a], 3473 [s]
AMgB…NaB	2377[a], 2340[a]	3575[a], 3591[a], 3444 [s], 3463 [s]
AMgB…KB	2365[a]	3575[a], 3431 [s], 3442 [s]
AMgB…ZnB	2565 [s], 2689[a]	3601[a],3471 [s], 3474 [s]
AMgB…MgB	2558 [s], 2669 [s]	3563[a],3440 [s]
AMgB…ALiB	2470[a]	3581[a], 3585[a], 3457 [s]
AMgB…ANaB	2588[a], 2334 [s]	3576[a], 3580[a], 3623[a], 3439 [s], 3449 [s], 3487 [s]
AMgB…AKB	2358 [s], 2367[a], 2573[a]	3574[a], 3616[a], 3441 [s], 3485 [s]
AMgB…AZnB	2499[a], 2602[a], 2524 [s]	3599[a], 3610[a], 3470 [s]
AMgB…AMgB	2441[a], 2410 [s]	3569[a], 3608[a], 3612[a], 3448 [s], 3479 [s], 3482 [s]

than the latter. It is revealed from Table III that the electron density at BCP decreases with increasing H···H bond distance emphasizing on the correlation between ρ at BCP and bond strength.[55]

Ellipticity (ε) measures the anisotropy of electron distribution at BCP, large value of ε indicates large deviation from sigma bond character and the least ellipticity ε of any non-bonded interaction reflects its strength.[54] Table III reveals that the maximum ellipticity value (3.099) was found in one of the DHB in AMgB···AMgB and the minimum value of ellipticity (0.032) was recorded for the DHB of AMgB···NaB complex which further reflects that the deviation in the electron distribution at BCP is comparatively larger in the former case and hence it may affect the strength of DHB in AMgB···AMgB system. Further, the observed values of ε were coexisted along with the H···H separation and electron density ρ at BCP in all the cases. For instance, the minimum value of ellipticity was found to be 0.032 which is coexisted along with the electron density value of 0.0128a. u. and the short H···H separation of 1.911 Å in non ammoniated metal complex AMgB···NaB.

Analysis of the QTAIM parameters such as the total electron energy density H(r), potential electron energy density V(r), and kinetic electron energy density G(r) at BCP provides the information for the easy identification of non covalent interaction. Since the sign of V(r) is always negative and for G(r) it is always positive, the sign of H(r) indicates whether V(r) or G(r) dominate in the bonding region. It is well known that the positive values of the total electron energy density H(r) at the BCP correspond to the non-covalent interaction and the negative values of H(r) indicates the presence of covalent interaction.[56] From Table III, it can be inferred that the observed values of H(r) are positive and it varies from 0.0008 to 0.0018a.u. which shows the existence of DHB.

After ammoniation, variations in the hydrogen atoms involved in DHB as well as increased number of DHBs were observed in all the ammoniated complexes. It follows from the topological parameters that all the chosen ammoniated complexes shows the presence of several short H···H contacts due to the inclusion of ammonia along with the considerable variation on the ρ and $(\nabla^2\rho)$ values of DHBs. For instance, ρ and $(\nabla^2\rho)$ values of DHB in AMgB···LiB are found to be 0.0109 and 0.0307a.u. respectively and it is increased to 0.0128 and 0.0419a.u. in its ammoniated complex of AMgB···ALiB. Moreover, the observed variations in ρ and $\nabla^2\rho$ values were correlated well with the H···H bond distance.

Besides, bifurcated DHBs were observed in AMgB···ALiB and AMgB···ZnB complexes with the presence of (3, −1) bond critical point along with the positive H(r) and $(\nabla^2\rho)$ value. Among the observed bifurcated bonds one of the H···H contact is longer and weaker than linear H···H interactions. In conjunction with this statement, one of the H···H contact in bifurcated HB observed in AMgB···ALiB has large ellipticity value (1.076), longer H···H separation (2.0281) and lower value of electron density at BCP than the other H···H contact which can be readily seen from the Table III. The same trend has been followed by the bifurcated DHBs observed in AMgB···ZnB complex.

In summary, the calculated topological parameters confirm the presence of DHBs in the considered complexes with positive H(r), Laplacian and electron density values. The introduction of NH_3 in the MB systems decreases the electron density ρ at BCP of B-H covalent bond and it increases the electron density at H···H interactions considerably while compared to non-ammoniated systems. Such a decrease in the electron density of ammoniated complexes can contribute significantly in weakening of the B-H bonds and strengthening of DHB, which possibly might be responsible for the easy dehydrogenation and extraction of H_2 under low temperature conditions.

Bader charge analysis.—In order to understand the charge transfer between a protic hydrogen ($N–H^{\delta+}$) and a hydridic hydrogen ($^{\delta-}$H-B) and electron distribution around the atoms, we have computed the Bader charges of Hydrogen atoms that involved in DHB interactions. Bader charge calculation is based on the number of electrons in AIM basin, and the difference in nuclear charge and AIM population yields the Bader charge.[42] In this study Bader charge calculation of all the AMgB···MB and AMgB···AMB complexes were performed by topological analysis of charge density using Multiwfn and the results were tabulated in Table IV. It is observed from the tabulated results that the Bader charge on hydrogen atoms that involved in the dihydrogen bonding exhibit the presence of both the protic hydrogen, $H^{\delta+}$ in NH_3 and hydridic hydrogen $H^{\delta-}$ in BH_4. From the sign and amount of charge accumulated on the H atoms, one can say that nearly −0.69e is accepted in B-H bonding since the sign –ve (atoms that accept electrons in general are indicated by –ve sign on the accumulated charge). Similarly, +0.44e electrons are donated by H atom in N-H bonding as the atoms that giving away electrons to the bonding is usually represented by +ve sign on the accumulated charge. In this way one can mention that the H atom bonded to B accepts nearly ∼−0.7e and donates +0.4e to the N atom in N- $H^{\delta+}$ bond. Further, the charge accumulation on the H atoms varies from ∼−0.69 to −0.73e and +0.44e to +0.47e in the AMgB···MB (Li, Na, K, Mg and Zn) complexes.

In order to understand the charge transfer, charge accumulation on $H^{\delta+}$ and $H^{\delta-}$ atoms involved in DHBs were noted before and after H···H bond formation. After DHB formation, charge accumulation on $H^{\delta+}$ increased in all the considered complexes and hence it reflects that significant amount of charge is donated towards H···H formation. At the same time, charge accumulation on $H^{\delta-}$ decreased in alkali metals and increased in both, the chosen alkaline and the transition metal complexes which further confirm the charge contribution by $H^{\delta-}$ atoms during DHB formation. For instance, in alkali metal complexes AMgB···MB, (M = Li, Na and K) charge distribution on the hydrogen atom ($H^{\delta+}$) bonded to nitrogen is found as +0.45e, +0.46e and +0.46e and it increases in the ammoniated complexes, where the values were found to be +0.46e, +0.47e and +0.47e respectively. Meanwhile, charge distribution around the hydrogen atom ($H^{\delta-}$) bonded to boron shows considerable

Table III. Topological Properties (in a.u.) of Amine metal borohydride complexes optimized at MP2/6–311++G level calculations.**

Amine Metal Borohydride Complexes	H···H distance (Å)	Electron density ρ (au)	Ellipticity ε	Laplacian($\nabla^2\rho$) (a.u.)	Total electron energy density H(r) (a.u.)	Potential energy V(r) (a.u.)
AMgB··· LiB	2.006, 1.998	0.0109, 0.0128	0.092, 0.301	0.0307, 0.0415	0.00087, 0.00179	−0.0059, −0.0068
AMgB···NaB	1.9108, 1.8719	0.0128, 0.0159	0.032, 0.142	0.0360, 0.0493	0.00115, 0.00175	−0.0067, −0.0088
AMgB···KB	1.8902, 1.9515	0.0155, 0.0119	0.231, −4.581	0.0474, 0.0519	0.00168, 0.00176	−0.0085, −0.0094
AMgB···ZnB	2.0601, 1.9628	0.0109, 0.0129	0.211, 0.150	0.0350, 0.0409	0.00148, 0.00165	−0.0058, −0.0069
AMgB···MgB	1.8314	0.0166	0.209	0.0507	0.00182	−0.0090
AMgB···ALiB	2.0111, 2.0281	0.0131, 0.0129	0.875, 1.076	0.0423, 0.0419	0.00180, 0.04193	−0.0069, −0.0069
AMgB···ANaB	2.2019, 2.0205, 2.0204	0.0083, 0.0134, 0.0133	0.345, 2.712	0.0267, 0.0442, 0.0437	0.00116, 0.00182, 0.00179	−0.0044, −0.0074, −0.0073
AMgB···AKB	2.0816, 1.8690, 1.8979	0.0099, 0.0163, 0.0160	0.217, 0.237, 0.405	0.0310, 0.0499, 0.0499	0.00139, 0.00168, 0.00173	−0.0050, −0.0091, −0.0090
AMgB···AZnB	2.1555, 2.1248, 1.9389, 2.0202	0.0105, 0.0104, 0.0119, 0.0117	0.409, 0.469, 0.049, 0.342	0.0357, 0.0339, 0.0356, 0.0386	0.00164, 0.00132, 0.00146, 0.00146	−0.0056, −0.0058, −0.0059, −0.0067
AMgB···AMgB	1.8749, 2.1202, 2.1584	0.0153, 0.0097, 0.0092	0.357, 0.905, 3.099	0.0476, 0.0322, 0.0335	0.00179, 0.00145, 0.00164	−0.0083, −0.0052, −0.0051

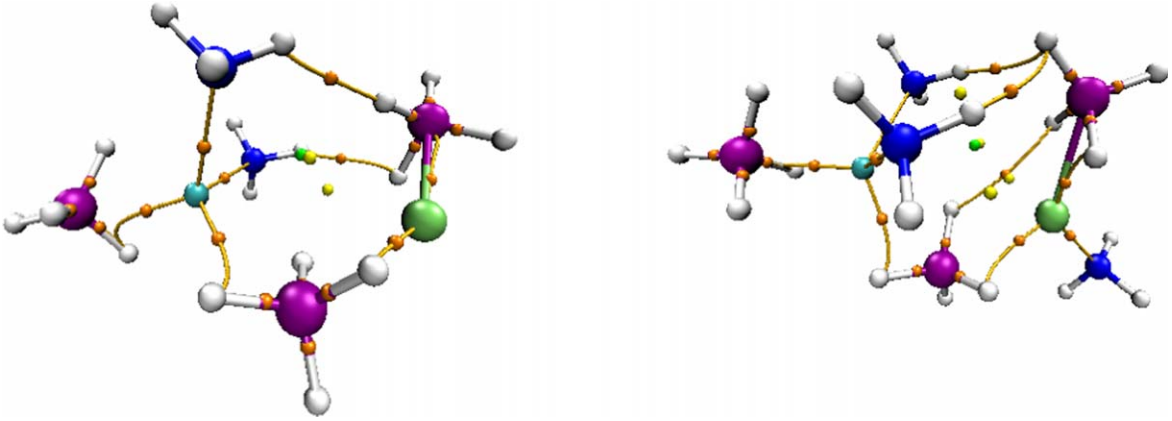

Figure 2. QTAIM molecular graph of AMgB···LiB and AMgB···ALiB complexes. Atom colours: Ash = H, Purple = B, Dark blue = N, Green = Li, Cyan = Mg and small orange sphere = BCP.

Table IV. Bader Charge (BC) analysis in e for AMgB···MB and AMgB···AMB complexes obtained at MP2/6–311++G level of theory.**

AMgB···MB Complexes	Bader Charge	AMgB···AMB Complexes	Bader Charge
AMgB···LiB $H^{\delta+}$ $H^{\delta-}$	0.4550, −0.7295	AMgB···ALiB $H^{\delta+}$ $H^{\delta-}$	0.4625, −0.7092
AMgB···NaB $H^{\delta+}$ $H^{\delta-}$	0.4629, −0.7315	AMgB···ANaB $H^{\delta+}$ $H^{\delta-}$	0.4677, −0.7386
AMgB···KB $H^{\delta+}$ $H^{\delta-}$	0.4695, −0.7333	AMgB···AKB $H^{\delta+}$ $H^{\delta-}$	0.4713, −0.7329
AMgB···ZnB $H^{\delta+}$ $H^{\delta-}$	0.4415, −0.6955	AMgB···AZnB $H^{\delta+}$ $H^{\delta-}$	0.4409, −0.6991
AMgB···MgB $H^{\delta+}$ $H^{\delta-}$	0.4415, −0.6955	AMgB···AMgB $H^{\delta+}$ $H^{\delta-}$	0.4688, −0.7221

decrement in the order of 0.007e to 0.02e. In the case of ZnB, charge accumulation on the $H^{\delta+}$ atom is decreased by the amount of 0.0008e and charge on $H^{\delta-}$ increases in magnitude by the amount of 0.036e due to the inclusion of NH_3 group. Wherein, ammoniation of MgB complex increases the charge accumulation on both the $H^{\delta+}$ and $H^{\delta-}$ hydrogen atoms from 0.02e to 0.03e. Hence, it is observed from the results that the addition of ammonia group and varying the interacting metal (AMgB···MB) from Li to Zn influence the charge transfer considerably.

Molecular electrostatic potential analysis.—MESP is used to visualize the charge distribution around the molecular interactions especially in non-covalent interactions. Several studies have been reported the importance of DHB interactions in cluster formation with the help of MESP parameters.[47,57,58] The role of electrostatics of DHB interactions and charge delocalization in determining the structural stability of ammonia borane cluster formations has been explored using MESP parameters.[57] Molecular interactions and the charge distributions of the considered complexes are visualized in MESP analysis using MP2 level of theory at 6–311++G** and given in the supporting information (Fig. S2). Due to the difference in the electronegativity values of B, N and H atoms, H atom in the N–H bonding exhibits strongly positive electrostatic potential at the end of the N–H bond and H atom in the B–H bonding exhibits strongly negative electrostatic potential at the end of the B–H bond. In general the positive potential at the ends of N–H suggest its ability to attract negative regions of the other interacting molecule. This has been observed with the positive electrostatic potential (red coloured region) around the N–H group and the negative regions(blue coloured region) of electrostatic potential around the B-H group that further confirms the presence of inter molecular interaction between N–$H^{\delta+}$ and $^{\delta-}$H–B in all the chosen complexes.

Energy decomposition analysis.—Energy Decomposition analysis (EDA) of the complexes calculated at MP2 level is displayed in Table V. The total interaction energy can be decomposed into three terms namely, electrostatic interaction between the interacting fragments ΔE_{elstat}, the exchange repulsion between the fragments due to Pauli's repulsion ΔE_{exch} and ΔE_{orb} the energy gain due to orbital interaction term. Among this three terms, ΔE_{elstat} and ΔE_{orb} terms are usually attractive whereas ΔE_{exch} is repulsive in nature.[46] It is noted from the Table V that the steric component of the interaction energy term has negative values for alkali metal borohydride systems AMgB···MB (M = Li, Na and K) which results in the predominating nature of electrostatic attraction when compared with the exchange term. In addition, orbital interaction term of these complexes also has negative value that shows the nature of interaction between the orbital of two fragments were attractive. Hence the interactions between the aforementioned complexes were determined by electrostatic as well as the orbital interaction term. In the case of Mg and Zn, the orbital interaction energy term is higher than that of the total interaction energy and hence it can be concluded that the stability of these complexes are governed by the orbital interaction term. Dispersion interaction term of EDA analysis was calculated to know about the role of dispersion interaction in stability determination. It follows from the Table V that the ΔE_{disp} term of the alkali metal borohydride complexes AMgB···MB (M = Li, Na and K) were found to be −7.42 kcal mol^{-1}, −2.49 kcal mol^{-1} and −2.17 kcal mol^{-1} respectively. Whereas, ΔE_{disp} values were calculated as −2.9 kcal mol^{-1} and −3.13 kcal mol^{-1} for AMgB···ZnB and AMgB···MgB complexes. Among the alkali metal complexes, LiB system has greater value and ΔE_{disp} term follows the trend Li<Na<K and ΔE_{disp} value of MgB is comparatively greater than that of ZnB (−2.9). It follows from the table that the ΔE_{disp} term has significant role in determining the structural stability.

After ammoniation, steric component of the interaction energy term in alkali metal borohydride system were found to be reduced by the amount of −3.04, −1.82 and −0.17 kcal mol^{-1} for the systems AMgB···ALiB, AMgB···ANaB and AMgB···AKB respectively. However, the ΔE_{disp} term of the aforementioned complexes were increased after ammoniation by the order of −1.03, −0.41 and −0.43 respectively. Wherein, AMgB···AZnB and AMgB···AMgB complexes show considerable decrement in the values of ΔE_{disp} term by the order of 0.83 and 2.61 kcal mol^{-1} respectively. Since the largest contribution to the interaction energy of AMgB···AZnB and

Table V. Energy Decomposition Analysis (EDA in kcal mol^{-1}) of dihydrogen bonded Amine metal borohydride complexes obtained by MP2/6–311++G and HF/6–311++G** level of theories.**

Amine Metal Borohydride Complexes	ΔE_{HF}	ΔE_{MP2}	$\Delta E_{(exch+elstat)}$	ΔE_{orb}	ΔE_{disp}
AMgB··· LiB	−23.41	−30.83	−17.53	−13.30	−7.42
AMgB···NaB	−24.12	−26.61	−14.12	−12.49	−2.49
AMgB···KB	−24.74	−26.91	−16.49	−10.42	−2.17
AMgB···ZnB	−14.64	−17.54	20.99	−38.53	−2.9
AMgB···MgB	−17.49	−20.62	8.06	−28.68	−3.13
AMgB···ALiB	−19.41	−27.86	−14.49	−13.37	−8.45
AMgB···ANaB	−22.83	−25.73	−12.3	−13.43	−2.9
AMgB···AKB	−24.86	−27.43	−16.32	−11.11	−2.6
AMgB···AZnB	−14.13	−16.20	−7.48	−8.72	−2.07
AMgB···AMgB	−14.58	−15.10	−7.88	−7.22	−0.52

AMgB···AMgB complexes, is given by both the electrostatic and orbital interactions, the dispersion term provides only less contribution. However, the effect of ammoniation process turns the steric term in the above mentioned system into attractive and reduces the orbital contribution, which may be due to spatial orientation of the interacting metal atoms (Refer Fig. 1). Hence, it explains why these two systems posses comparatively less dispersion energies. At this point, we concluded that ammoniation significantly alter the stability of the interaction between the chosen complexes through non bonded dihydrogen bonding since the ΔE_{disp} term increases after ammoniation in alkali metals. Among all the complexes, ALiB···AMgB shows greater value of ΔE_{disp} term and AMgB···AMgB has lower ΔE_{disp} value.

Interaction energy.—Interaction energy of the complexes calculated at MP2/6–311++G** level theory is listed in Table VI. For better understanding total energy and BSSE corrected energies were listed in Table SIII (supporting information). The highest interaction energy of ∼−30.83 kcal mol^{-1} is observed for the complex of AMgB···LiB whereas, the least interaction energy of −15.10 kcal mol^{-1} is observed for AMgB···AMgB complex. Upon ammoniation, alkali metal borohydride complexes show decreased amount of interaction energy, which might be due to the absence of ionic (M^+-H^-) interaction between the hydride ligand of BH_4 moiety in AMgB and the alkali metal ion (Li^+ an Na^+) that present in the non ammoniated metal borohydride complexes (Refer Fig. 1). Say for instance, due to the absence of Li-H interaction, AMgB···ALiB exhibits the decreased value in its interaction energy from −30.83 to -27.86 kcal mol^{-1} which is in agreement with the EDA analysis that shows presence of lower value of electrostatic attraction ΔE_{elstat} term in AMgB···ALiB. In the case of transition and alkaline metals, interaction energy of AMgB···MgB and AMgB···ZnB complexes are found to be −20.62 and −17.54 kcal mol^{-1} and it is reduced to −15.10 and −16.20 kcal mol^{-1} after ammoniation. It is further in line with the EDA analysis since orbital interaction term has greater value in both the AMgB···MgB and AMgB···ZnB systems due to the spatial orientation of the two interacting systems. After ammoniation interaction energies of ammoniated Mg and Zn borohydride complexes were reduced considerably which may be due to lower orbital interaction term. Even though ammoniation reduces the interaction energy term, alkali metal complexes follow the same trend as the values changes as Li < K < Na in both the cases before and after ammoniation. Further, the process of ammoniation alters the electrostatic attraction term as well as dispersive interaction term in alkali metal system significantly and the orbital interaction term changes much in response to the ammoniation process in the case of AMgB···MgB and AMgB···ZnB systems.

In general, interaction energy values are in line with the geometrical parameters such as H···H and M···H distances. It is evident from Table VI that the values of interaction energies were not correlated with the H···H distances. For example, AMgB···LiB posses higher interaction energy value (−30.83 kcal mol^{-1}) with H···H distances in the range of 2 Å. In spite of shorter H···H contacts in the order of ∼1.8 Å, comparatively lower interaction energy of −26.91 kcal mol^{-1} is recorded for AMgB···KB. Since the nature of interacting metal is different for different complexes, contribution to the interaction energy of AMgB···MB (Li, Na, K, Mg and Zn) systems varies significantly. For instance, all the three terms namely $\Delta E_{exch+elstat}$, ΔE_{orb} and ΔE_{dis} had greater values in AMgB···LiB interaction which results in high interaction energy, even though AMgB···NaB has comparatively short H···H contacts, the calculated interaction energy is −26.61 kcal mol^{-1}. This could be explained with the help of decremented contribution observed from $\Delta E_{exch+elstat}$, ΔE_{orb} and ΔE_{dis} terms when the interacting metal is changed from Li to Na. In the case of AMgB···LiB, value of $\Delta E_{exch+elstat}$ term was found to be −17.53 kcal mol^{-1} and it is reduced to −14.12 kcal mol^{-1} in AMgB···NaB. Since the contribution of $\Delta E_{exch+elstat}$ towards the interaction energy is comparatively less in AMgB···NaB, which further reflects lesser interaction energy. On the whole, it can be understood from the interaction energy calculations that both the nature of interacting metal atom and the ammoniation process strongly influences the interactions between the chosen complexes since it alters the interaction energy values.

Table VI. Interaction energies of dihydrogen bonded Amine metal borohydride complexes obtained by MP2/6–311++G level of theory.**

Amine metal borohydride complexes	Interaction energy E_{int} kcal mol^{-1}
AMgB··· LiB	−30.83
AMgB···NaB	−26.61
AMgB···KB	−26.91
AMgB···ZnB	−17.54
AMgB···MgB	−20.62
AMgB···ALiB	−27.86
AMgB···ANaB	−25.73
AMgB···AKB	−27.43
AMgB···AZnB	−16.21
AMgB···AMgB	−15.10

Conclusions

Dihydrogen bond network exist in the complexes of AMgB with various metal borohydrides along with their ammoniates were investigated using MP2 level of theory. The H···H distance and topological parameters such as electron density (ρ), Laplacian of electron density ($\nabla^2\rho$) and total electron density H(r) exhibits the presence of DHBs in all the optimized structures. It is well established by various experimental studies that the presence of both positively charged $H^{\delta+}$ and negatively charged $H^{\delta-}$ within the same structural framework could improve the volumetric hydrogen storage capacity. Such DHB interactions between the networks of $N–H^{\delta+}$ and $^{\delta-}H–B$ in AMgB systems are responsible for many interesting properties like structural flexibility, ionic conductivity and improved dehydrogenation properties. Formation of complex hydrides by adding different metal borohydrides might influences the dehydrogenation property of AMgB since it increases the number of DHBs into the structure. In conjunction with this statement, nature of DHB interactions between AMgB and various MB (M = Li, Na, K, Mg and Zn) along with its ammoniates results in improved H···H interaction which is crucial for H_2 evolution.

Inclusion of amino group significantly influences the electron distribution at H···H interaction site further confirms the role of ammoniation process in DHB formation. Charge transfer that occurs between the $H^{\delta+}$ and $H^{\delta-}$ atoms found to determine the nature of DHB present, which is in agreement with the QTAIM results. EDA result reflects the ammoniation effect since the ΔE_{disp} term increases after ammoniation in alkali metals. Moreover, EDA and interaction energy results were calculated and are found to correlate well with the geometrical parameters and ρ values of H···H interactions. Adding metal borohydride to AMgB is an effective approach for improving the dehydrogenation as well as for the suppression of NH_3 emission in AMgB complexes. However, our results suggest that the process of adding amine alkali metal borohydrides to AMgB increases charge distribution around the dispersion interaction which plays a vital role in hydrogen evolution process. Hence, this study gives a new idea to understand the impact ammoniation process on the DHB interactions found in the complex hydride systems. By combining the results of all the chosen complex hydrides, significantly improved dehydrogenation property is expected for AMgB···LiB and AMgB···ALiB since it exhibits the strong DHB among all other complexes.

Acknowledgments

I thank the Management and Principal of Dr. N.G.P Arts and Science College for providing their support to carry out my research work.

ORCID

Praveena Gopalan https://orcid.org/0000-0001-7942-3150

References

1. J. Jiang, Q. Liang, S. Zhang, R. Meng, C. Tan, Q. Yang, X. Sun, H. Ye, and X. Chen, *J. Mater. Chem. C*, **4**, 8962 (2016).
2. N. V. Belkova, L. M. Epstein, O. A. Filippov, and E. S. Shubina, *Chem. Rev.*, **116**, 8545 (2016).
3. Y. Yao, X. Yong, J. S. Tse, and M. J. Greschner, *J. Phys. Chem. C*, **118**, 29591 (2014).
4. C. A. Morrison and M. M. Siddick, *Angew. Chem.- Int. Ed*, **43**, 4780 (2004).
5. X. Chen, J. C. Zhao, and S. G. Shore, *Acc. Chem. Res.*, **46**, 2666 (2013).
6. R. Custelcean and J. E. Jackson, *J. Am. Chem. Soc.*, **120**, 12935 (1998).
7. I. E. Golub, O. A. Filippov, E. I. Gutsul, N. V. Belkova, L. M. Epstein, A. Rossin, M. Peruzzini, and E. S. Shubina, *Inorg. Chem.*, **51**, 6486 (2012).
8. I. E. Golub, O. A. Filippov, N. V. Belkova, L. M. Epstein, and E. S. Shubina, *J. Organomet. Chem.*, **865**, 247 (2018).
9. I. E. Golub, O. A. Filippov, N. V. Belkova, L. M. Epstein, A. Rossin, M. Peruzzini, and E. S. Shubina, *Dalton Trans.*, **45**, 9127 (2016).
10. S. Qiu, H. Chu, Y. Zou, C. Xiang, F. Xu, and L. Sun, *J. Mater. Chem. A*, **5**, 25112 (2017).
11. E. Jeon and Y. W. Cho, *J. Alloys Compd.*, **422**, 273 (2006).
12. Z. Z. Fang, L. P. Ma, X. D. Kang, P. J. Wang, P. Wang, and H. M. Cheng, *Appl. Phys. Lett.*, **94**, 1 (2009).
13. F. C. Gennari, L. Fernández Albanesi, and I. J. Rios, *Inorganica Chim. Acta*, **362**, 3731 (2009).
14. L. V. Titov and E. R. Eremin, *Bulletin of the Academy of Sciences of the USSR Division of Chemical Science*, **24**, 1095 (1975).
15. P. Choudhury, S. S. Srinivasan, V. R. Bhethanabotla, Y. Goswami, K. McGrath, and E. K. Stefanakos, *Int. J. Hydrog. Energy*, **34**, 6325 (2009).
16. R. Mohtadi, A. Remhof, and P. Jena, *J. Phys. Condens. Matter*, **28**, 353001 (2016).
17. K. T. Møller, D. Sheppard, D. B. Ravnsbæk, C. E. Buckley, E. Akiba, H. W. Li, and T. R. Jensen, *Energies*, **10**, 1645 (2017).
18. D. J. Durbin and C. Malardier-Jugroot, *Int. J. Hydrog. Energy*, **38**, 14595 (2013).
19. G. Soloveichik, J. H. Her, P. W. Stephens, Y. Gao, J. Rijssenbeek, M. Andrus, and J. C. Zhao, *Inorg. Chem.*, **47**, 4290 (2008).
20. L. H. Jepsen, M. B. Ley, Y. Filinchuk, F. Besenbacher, and T. R. Jensen, *ChemSusChem*, **8**, 1452 (2015).
21. Y. Yan, J. B. Grinderslev, Y. S. Lee, M. Jørgensen, Y. W. Cho, R. Černý, and T. R. Jensen, *Chem. Comm*, **56**, 3971 (2020).
22. Y. Yan, W. Dononelli, M. Jørgensen, J. B. Grinderslev, Y. S. Lee, Y. W. Cho, R. Černý, B. Hammer, and T. R. Jensen, *Phys. Chem. Chem. Phys.*, **22**, 9204 (2020).
23. I. F. David William, S. R. Johnson, D. M. Royse, M. Sommariva, C. Y. Tang, F. P. A. Fabbiani, M. O Jones, and P. P. Edwards, *J. Chem*, **4**, 849 (2009).
24. Y. Zhang, Y. Liu, X. Zhang, Y. Li, M. Gao, and H. Pan, *J. Phys. Chem. C*, **119**, 24760 (2015).
25. L. H. Jepsen, M. B. Ley, R. Černý, Y. S. Lee, Y. W. Cho, D. Ravnsbæk, F. Besenbacher, J. Skibsted, and T. R. Jensen, *Inorg. Chem.*, **54**, 7402 (2015).
26. Y. Yang, Y. Liu, Y. Li, M. Gao, and H. Pan, *J. Mater. Chem. A*, **3**, 570 (2015).
27. X. Zheng, G. Wu, W. Li, Z. Xiong, T. He, J. Guo, H. Chen, and P. Chen, *Energy Environ. Sci.*, **4**, 3593 (2011).
28. Y. Guo, Y. Jiang, G. Xia, and X. Yu, *Chem. Comm*, **48**, 4408 (2012).
29. W. Sun, X. Chen, Q. Gu, K. S. Wallwork, Y. Tan, Z. Tang, and X. Yu, *Chem. Eur. J.*, **18**, 6825 (2012).
30. Y. Yang, Y. Liu, Y. Li, M. Gao, and H. Pan, *J. Phys. Chem. C*, **117**, 16326 (2013).
31. Q. Gu, L. Gao, Y. Guo, Y. Tan, Z. Tang, K. S. Wallwork, F. Zhang, and X. Yu, *Energy Environ. Sci.*, **5**, 7590 (2012).
32. L. H. Jepsen, Y. S. Lee, R. Černý, R. S. Sarusie, Y. W. Cho, F. Besenbacher, and T. R. Jensen, *ChemSusChem*, **8**, 3472 (2015).
33. F. Yuan, Q. Gu, X. Chen, Y. Tan, Y. Guo, and X. Yu, *Chem. of Mater*, **24**, 3370 (2012).
34. A. Staubitz, A. P. M. Robertson, and I. Manners, *Chem. Rev.*, **110**, 4079 (2010).
35. M. Paskevicius, L. H. Jepsen, P. Schouwink, R. Černý, D. B. Ravnsbæk, Y. Filinchuk, M. Dornheim, F. Besenbacher, and T. R. Jensen, *Chem. Soc. Rev.*, **46**, 1565 (2017).
36. D. Parimala Devi, G. Praveena, and A. Abiram, *Chem Pap*, **74**, 1609 (2020).
37. E. Welchman and T. Thonhauser, *J. Mater. Chem. A*, **5**, 4084 (2017).
38. P. S. V. Kumar, V. Raghavendra, and V. Subramanian, *J. Chem Sci,*, **128**, 1527 (2016).
39. Y. Nakamori, K. Miwa, A. Ninomiya, H. Li, N. Ohba, S. I. Towata, A. Züttel, and S. I. Orimo, *Phys Rev. B, Condens. Matter*, **74**, 1 (2006).
40. G. A Zhurko and D. A Zhurko et al., Chemcraft - graphical software for visualization of quantum chemistry computations, https://www.chemcraftprog.com.
41. N. S. Venkataramanan, A. Suvitha, H. Mizuseki, and Y. Kawazoe, *Int. J. Quantum Chem.*, **113**, 1940 (2013).
42. T. Lu and F. Chen, *J. Comput. Chem.*, **33**, 580 (2012).
43. S. F. Boys and F. Bernardi, *Mol. Phys.*, **19**, 553 (1970).
44. M. von Hopffgarten and G. Frenking, *Wiley Interdiscip. Rev. Comput. Mol. Sci*, **2**, 43 (2012).
45. G. W. T. M. J. Frisch et al., (Gaussian, Inc, Wallingford CT)*Revision B.01* (2009).
46. R. Pawar and V. Subramanian, *Comput. Theor. Chem*, **1165**, 1 (2019).
47. S. R. Gadre, C. H. Suresh, and N. Mohan, *Molecules*, **26**, 1 (2021).
48. L. Pauling, *J. Am. Chem. Soc.*, **69**, 542 (1947).
49. P. Vajeeston, P. Ravindran, A. Kjekshus, and H. Fjellv, *J. Alloys Compd.*, **406**, 377 (2005).
50. S. Najiba and J. Chen, *PNAS*, **109**, 19140 (2012).
51. K. M. Dreux, L. E. McNamara, J. T. Kelly, A. M. Wright, N. I. Hammer, and G. S. Tschumper, *J. Phys. Chem. A*, **121**, 5884 (2017).
52. T. Kar and S. Scheiner, *J. Chem. Phys.*, **119**, 1473 (2003).
53. W. Humphrey, A. Dalke, and K. Schulten, *VMD - Visual Molecular Dynamics', J. Molec. Graphics*, **14.1**, 33 (1996).
54. P. L. A. Popelier, *J. Phys. Chem. A*, **102**, 1873 (1998).
55. E. Espinosa, E. Molins, and C. Lecomte, *Chem. Phys. Lett.*, **285**, 170 (1998).
56. K. S. Sandhya, G. S. Remya, and C. H. Suresh, *J. Chem. Sci.*, **130**, 1 (2018).
57. K. P. Vijayalakshmi and C. H. Suresh, *J. Phys. Chem. A*, **121**, 2704 (2017).
58. N. Mohan and C. H. Suresh, *Int. J. Quantum Chem.*, **114**, 885 (2014).